PCCP

Accepted Manuscript

ROYAL SOCIETY OF CHEMISTRY

www.rsc.org/pccp

Cite this: DOI: 10.1039/c0xx00000x

www.rsc.org/xxxxxx

ARTICLE TYPE

Temporary Anion States of p-Benzoquinone: Shape and Core-Excited Resonances

Hsiu-Yao Cheng* and Yu-Shiuan Huang

Received (in XXX, XXX) Xth XXXXXXXXX 20XX, Accepted Xth XXXXXXXXX 20XX

DOI: 10.1039/b000000x

The studies of shape and core-excited resonances are essential in the bonding and electronic processes of quinones. So far, the experimental results of temporary anion states for p-benzoquinone cannot be fully ascertained computationally. In this paper, both resonances of p-benzoquinone are investigated via stabilization method (SM). For shape resonances, the stabilized Koopmans theorem is adopted in the framework of long range corrected density functional theory (LC-DFT). As for core-excited resonances, the SM coupled with long range corrected time-dependent density functional theory (LC-TDDFT) is employed. The resonance energies and lifetimes are then estimated via an analytic continuation procedure in conjunction with the stabilization plots. Using this novel combination, previous experimental results of temporary anion states can be successfully identified. It is believed that this novel approach can be an accurate and efficient methodology in the study of temporary anion states of quinones.

1. Introduction

Quinones and their derivatives have aroused considerable scientific interest due to their importance in the diverse areas of synthetic and environmental chemistry, biology and pharmacology.[1-5] For instance, quinone based molecular receptors can be used for recognition of anions and metal ions.[1] In addition, quinones can also enhance dechlorination of carbon tetrachloride by *Geobacter sulfurreducens*.[2] Quinones extracted from rhubarb are found to have proficient ability in grabbing and releasing electrons and can be used in metal-free flow battery technology for large-scale energy storage.[3] It is also well-known that quinones can function as the primary electron and proton carriers in basic metabolic processes such as respiration and photosynthesis.[4] Natural quinones and many of their synthetic derivatives have a variety of biological activities that can inhibit the growth of tumors pharmacologically.[5] It is believed that p-benzoquinone (p-BQ), the prototypical quinone species, plays an important role in electron-accepting ability.

From the brief introduction of the previous paragraph, it is crucial to understand the so-called temporary anion states (TASs) of p-BQ. The important reason is that TASs are essential in the study of bonding and electron transfer processes of quinones. TASs can, in general, be divided into two categories according to how the extra electron attaches to their parent state.[6] The first category of "shape resonance" (SR) stands for the case that an extra electron is attached to an unfilled valence orbital of the neutral ground state. As to the second category of "core-excited resonance", it is associated with the electron attachment to an excited state of the neutral molecule. The second category can be further divided into two types according to their energy with respect to the excited state of the neutral molecule. Type I or Feshbach resonance lies energetically below its parent state, while Type II resonance or core-excited shape resonance lies above its parent state.

To gain a fundamental understanding of the TASs of p-BQ, a combination of experimental and computational methods is required. Cooper et al.[7] observed 3 peaks of TASs at 0.70, 1.35, and 1.90 eV using the SF_6-scavenger technique. A 4th peak at 4.35 eV could not be definitely assigned. Based on electron transmission spectroscopy measurement, Modelli and Burrow[8] assigned 4 TASs at 0.69, 1.41, 2.11, and 4.37eV. A weak 5th broad band at 5.8 eV was also observed. Allan[9] has identified 4 TASs at 0.72, 1.43, and 2.15 eV using electron energy loss spectroscopy as well as trochoidal electron spectrometer. Out of these controversial assignments, the multi-configurationally second-order perturbation CASPT2 calculations by Pou-Amérigo et al.[10] and the symmetry adapted cluster-configuration interaction (SAC-CI) by Honda et al.[11] have identified 3 TASs around 0.7, 1.4 and 2.0 eV. However, the assignment of higher TASs of p-BQ is still an open problem.

As a matter of fact, the computation on the energies of TASs is arduously challenging. First of all, proper size of basis set containing diffuse functions is required to describe the electron densities in the TASs. To deal with the variational collapse of TASs onto the neutral plus a discretized approximate continuum[13,14] (DC) solutions, the stabilization method (SM) pioneered by Taylor and Hazi[15] can be invoked. In particular, the vertical attachment energies (AEs) for temporary anion computed via the stabilized Koopmans' theorem[13,14] (SKT) method (i.e., the SM coupled with Koopmans' theorem[16]) is related to the energies of the stabilized virtual orbitals of the neutral molecules. The

SKT can be used within the frameworks of Hartree-Fock or density functional theory[17] (DFT). Notice that when the DFT is used, the Kohn-Sham virtual orbitals are less diffuse than those of Hartree-Fock.[18] Yet, many DFT potentials will not yield asymptotic behaviour properly and often underestimate the SR energies. Nevertheless, the problem, when using the DFT, can be remedied by using asymptotically corrected potentials.[19,20] As for core-excited resonances, their energies can be evaluated by comparing the energies of the excited vertical anion states with that of the ground neutral state.[21] However, the excited anion states could be derived from the excitations of an electron to either unfilled orbital or DC solutions. Hence, their energies may change when the basis set is varied. Consequently, these two types of excitations have to be differentiated via the SM.

The aim of this paper is to settle the assignment problem of TASs of p-BQ. First, we will focus on the SRs, and then the core-excited resonances. In particular, the SM using LC-DFT and LC-TDDFT will be adopted in this investigation. Their resonance energies and lifetimes will be calculated via analytic continuation method in conjunction with stabilization plots (SPs). Finally, the results of stabilization calculations will be compared with previous studies.

2. Computational Method

In this paper, six different basis sets of Gaussian-type, A1, A2, B1, B2, C1, and C2 are used in the stabilization calculations. The reason for using the shorthand notation A1,…, C2 in naming is because the conventional standard basis set has to undergo a scaling procedure. For instance, the basis set A1 stands for the 6-311++G(d,p) basis set with scaling of the exponents in the diffuse "+" functions on all atoms. Here, as it is well-known, that the first + represents the diffuse sp functions on C and O atoms and the second + stands for the s function on H atom. For the scaling procedure for the basis set A1, we mean that the exponents of diffuse "++" functions will be multiplied by a scale factor α. As for the other basis sets, A2 is formed by firstly augmenting the 6-311+G(d,p) basis set with the diffuse sp function on C and O atoms and then simultaneously scaling the exponents of the two most diffuse sets of sp functions on C and O atoms. The exponents of augmented diffuse sp functions are 0.01460 and 0.02817 for the C and O atoms, respectively. B1 is formed by replacing the outermost diffuse p functions on the C and O atoms of the lanl2dzdp[22] basis set with diffuse sp functions, which were scaled. B2 is formed by replacing the outermost diffuse p functions on the C and O atoms of the lanl2dzdp basis set with two diffuse sp functions with exponents of 0.03110 and 0.01037 on C and 0.06730 and 0.02243 on O, which were simultaneously scaled. C1 stands for the aug-cc-pvtz[23] basis set with scaling of the outermost diffuse s and p functions on the C and O atoms and the outermost s function on the H atom. Finally, C2 is formed by augmenting the C1 basis set with the diffuse p function on C and O with exponents of 0.01190 on C and 0.01991 on O, which were scaled. The purpose for such selection of six different basis sets is to understand the stability of stabilization calculations with respect to basis set variation.

In the present study, the SM that determines the eigenvalues of interest as a function of an adjustable factor α for the TASs is invoked. The SPs are obtained by graphing the calculated energies as a function of α. As the parameter α is varied, TA and DC solutions mix and avoided crossings (ACs) between two types of solutions may occur in SPs. In the calculation of resonance energies, the 'midpoint method' in Burrow et al.[24] will be adopted here, i.e., the energy of TAS is obtained by taking the average of two eigenvalues in the avoided crossing of closest approach at α_{ac}.[25] To estimate resonance energies (E_R) and widths (Γ), the calculated results of E(α) on the real axis will be extended via analytic continuation method into the complex plane from the ACs of the SPs. The method of analytic continuation has been used since the 1970s, various approaches have been proposed to extract parameters of resonances.[26] As to the procedure of analytic continuation in this study, the (i,i,i) generalized Padé approximants[26h-j] are employed by the following formula:

$$P(\alpha)\,E^2 + Q(\alpha)\,E + R(\alpha) = 0, \quad (1)$$

where

$$P(\alpha) = 1 + p_1\alpha + p_2\alpha^2 + \ldots + p_i\alpha^i, \quad (2)$$

$$Q(\alpha) = q_0 + q_1\alpha + q_2\alpha^2 + \ldots + q_i\alpha^i, \quad (3)$$

$$R(\alpha) = r_0 + r_1\alpha + r_2\alpha^2 + \ldots + r_i\alpha^i. \quad (4)$$

By substituting 3i+2 pairs of data points {E, α} into eq. (1)-eq. (4), the 3i+2 coefficients of these three polynomials can be determined from 3i+2 linear equations by standard matrix methods. Then, the Newton-Raphson procedure is used to solve $dE/d\alpha = 0$ to determine the stationary points, α_{stat}. The acquired values of α_{stat} are substituted into eq. (1)-eq. (4) to yield the corresponding stationary energies of $E_{stat}(\alpha_{stat})$. The complex resonance parameters are then determined by the real and imaginary parts at the above stationary point, $E_{stat}(\alpha_{stat}) = E_R - i\Gamma/2$. The width is associated with the lifetime τ via $\tau = \hbar/\Gamma$.

In the SKT computations for the SRs of p-BQ, the ωB97XD[27] and M11[28] LC functionals have been adopted. For comparison, the double-hybrid functional B2PLYPD3[29] that contains second-order perturbation corrections with Grimme's D3BJ dispersion is also included. In addition, the SM in conjunction with the electron-attached (EA) SAC-CI[30] and outer valence Green's function[31] correlated methods are also studied. The former will be denoted as S-EA SAC-CI and the latter as S-OVGF. In this paper, the EA-EOM-CCSD[32] will not be used because it suffers from the problem of non-convergence for small values of α in the stabilization calculations for p-BQ molecule.[33] In the same vein, neither the Hartree-Fock will be used since the energies of the unfilled orbitals would be too high.[18] As for the core-excited resonances, the same ωB97XD and M11 LC functionals have been chosen in the S-LC-TDDFT computations.[34] All calculations in this paper are performed using the Gaussian 09[35] program with geometric optimization of neutral p-BQ being carried out at the B3LYP/6-311++G(d,p) level under D_{2h} symmetry constraints. The optimized bond lengths of C=O, C=C, C-C, and C-H are 1.22, 1.34, 1.49, and 1.08 Å respectively. The calculated structural parameters are in good agreement with experimental structural parameters for the p-BQ.[36]

3. Results and Discussions

First, we will present results in the SKT calculations for the SRs of p-BQ using ωB97XD. In the D_{2h} point group, p-BQ has eight a_g, one b_{1g}, seven b_{1u}, one b_{2g}, five b_{2u}, four b_{3g}, and two b_{3u} occupied orbitals. Our symmetry in the labelling of the orbital is based on a molecular orientation with the x-axis being perpendicular to the molecular plane, and the z-axis lying along two carbonyl groups. The eight 2p orbitals of C and O atoms of p-BQ molecule can yield four π and four π* orbitals. According to our analyses for the π orbitals, the $1b_{3u}(\pi^+_u)$ is from the bonding interaction between two carbonyl $\pi^+_{C=O}$ and ethylene $\pi^+_{C=C}$ group orbitals. The $1b_{2g}(\pi^-_{CO})$ is primarily from the two $\pi_{C=O}$ and $1b_{1g}(\pi^+_{CC})$ from the two $\pi_{C=C}$ group orbitals. The $2b_{3u}(\pi^+_u)$ is predominantly from the antibonding interaction between two $\pi^+_{C=C}$ and $\pi^+_{C=O}$ group orbitals. As for the π* orbitals, the $2b_{2g}(\pi^{*-}_g)$ is primarily from the bonding interaction of the two $\pi^{*-}_{C=O}$ and $\pi^{*-}_{C=C}$ group orbitals. The $1a_u(\pi^{*-}_{CC})$ results from the two $\pi^{*-}_{C=C}$, and the $3b_{3u}(\pi^{*+}_{CO})$ is primarily from the two $\pi^{*+}_{C=O}$ group orbitals. The $3b_{2g}(\pi_g{}^{*-})$ is primarily from the antibonding interaction between two $\pi^{*-}_{C=O}$ and $\pi^{*-}_{C=C}$ group orbitals. Here, the superscripts + and - indicate the symmetry with respect to the x-y plane.

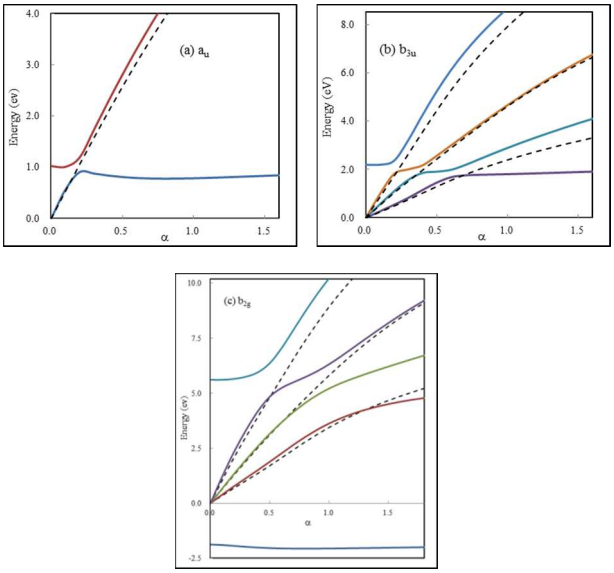

Fig. 1 SPs for p-BQ via SKT ωB97XD. Energies of (a) a_u, (b) b_{3u}, and (c) b_{2g} (solid curves) and the 1e DC (dashed curves) virtual orbitals as a function of α.

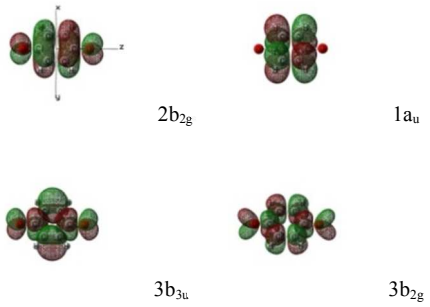

Fig. 2 Plots of the $2b_{2g}$, $1a_u$, $3b_{3u}$, and $3b_{2g}$ orbitals at α = 0.8 for p-BQ. The iso surface values are chosen to be 0.02 for all plots.

To discern the unfilled orbital and DC solutions of the p-BQ, the Schrödinger equation for one free electron (1e) in the absence of nuclear charges and other electrons as described by the molecular basis set is solved.[13c,d] Figure 1a-c shows the SPs of p-BQ for the a_u, b_{3u}, and b_{2g} virtual orbitals and the 1e DC solutions using the SKT ωB97XD method with basis set A1. The spectrum of eigenvalues in the SKT calculations consists of unfilled orbital and virtual DC solutions. One can determine the possible TASs by comparing the energies and characteristics of these two kinds of virtual orbitals with those of the 1e DC. In Fig. 1a, the energies for the first two ^2A_u eigenvalues are reported. The 1st and 2nd roots undergo an AC near $\alpha_{ac}(1,2) = 0.2$, indicating the presence of a TAS. The corresponding energy is 0.92 eV. In Fig. 1b, three ACs are from the couplings between $3b_{3u}$ orbital and the first three DC solutions. Their corresponding energies are 1.83 eV at $\alpha_{ac}(1,2) = 0.6$, 2.01 eV at $\alpha_{ac}(2,3) = 0.4$, and 2.09 eV at $\alpha_{ac}(3,4) = 0.2$. The mean value from each set will be defined as the energy of the TAS. Hence, the energy of the $3b_{3u}$ orbital is 1.98 eV. In Fig. 1c, the 1st root is primarily from the $2b_{2g}$ whose energy lies below zero (~-2.05 eV). The two ACs are from the couplings between $3b_{2g}$ orbitals and the 2nd and 3rd DC solutions, respectively. Their corresponding energies are 5.47 eV at $\alpha_{ac}(3,4) = 1.0$ and 5.61 eV at $\alpha_{ac}(4,5) = 0.6$. Thus the energy of the $3b_{2g}$ orbital is 5.54 eV. Figure 2 shows the $2b_{2g}$, $1a_u$, $3b_{3u}$, and $3b_{2g}$ orbitals for α = 0.8.

Table 1 reports the calculated AEs using various methods along with the experimental data for p-BQ. Notice that all basis sets contain polarization functions on H. The basis sets A1, C1, and C2 contain polarization functions and scaled diffuse function on H. As shown in Table 1, the AEs vary within 0.2 eV for each orbital for all basis sets. Hence, the SM results are reasonably stable with respect to the basis set variation. In Table 1, the increasing order of AEs of unfilled orbitals is $2b_{2g} < 1a_u < 3b_{3u} < 3b_{2g}$ for all stabilization calculations. For the $^2B_{2g}$ ground anion state, previous experimental and theoretical studies have indicated this lowest anion state is stable.[7,10-12] Our SKT ωB97XD and M11 calculated results on AEs (~ -1.8 – -2.1 eV) are in agreement with those of Cooper et al.[7] (-1.89 eV) using the cesium collisional ionization technique and Schiedt and Weinkauf[12a] (-1.86 eV) via photoelectron spectroscopy. Nevertheless, S-EA SAC-CI and S-OVGF approaches overestimate AEs (~ -1.0 – -1.2 eV) while SKT B2PLYP3D approach underestimates AEs (~ -2.2 eV). The first AE can also be obtained as the difference between the total energy of neutral and anion ground state, both in the optimized geometry of the neutral state. According to our study, the energies of the first vertical anion state relative to the neutral ground state with B3LYP calculations are -1.90, -1.85, and -1.86 eV using 6-311++G(d,p), lanl2dzdp, and aug-cc-pvtz basis sets, respectively. These calculated AEs are also in agreement with those of previous experimental studies.

Next, for the three unbound π* TASs, our SKT ωB97XD and M11 calculated AEs are in agreement with previous experimental data.[7-9] It is clear from Table 1 that the SKT ωB97XD and SKT M11 calculations generally yield better AEs as compared to those of the SKT B2PLYPD3, S-EA SAC-CI and S-OVGF methods. The AEs obtained from the S-OVGF method are larger than those obtained from the other methods (~ 1 eV). Notice that previous

assignments for TASs are not conformable among themselves. Based on comparison with calculated orbital energies, Cooper et al.[7] associated the resonances (0.7, 1.35, and 1.90 eV) determined from their SF_6-scavenger technique with ^2A_u, $^2B_{3u}$, and $^2B_{2g}$ SRs. They revised their assignments to $^2B_{3u}$, ^2A_u, and $^2B_{3u}$ resonances based upon optical study later on. Previous studies by Modelli and Burrow[8] associated the resonances at 0.69, 1.41 and 4.37eV observed in their electron transmission spectrum with $^2B_{3u}$, ^2A_u, and $^2B_{3u}$ SRs and those at 2.11 and 5.8 eV with core-excited resonances. Electron energy loss spectroscopy and electron transmission spectroscopy studies by Allen[9] attributed the resonances at 0.72, 1.43, and 2.15 eV as the $^2B_{3u}$, ^2A_u, and $^2B_{3u}$ SRs and the resonance around 4.37 eV as the $^3B_{3g}$ second π-π^* state. From the CASPT2 calculations, Pou-Amérigo et al. predicted ^2A_u, $^2B_{3u}$, and $^2B_{3u}$ resonances at 0.91, 1.31 and 1.87 eV (Table 7 of ref 10). Based on SAC-CI theoretical study, Honda et al. reported ^2A_u, $^2B_{3u}$, and $^2B_{3u}$ resonances at 0.83, 1.79, and 2.44 eV (Table 8 of ref 11). It is clear from Table 1 that our assignments of the two TASs, i.e., ^2A_u and $^2B_{3u}$, are in accordance with the results by Pou-Ame´rigo et al and Honda et al. It is noteworthy that for the experimental data around 1.35-1.43 and 4.2-4.37 eV, they are not corresponding to SRs in our results. It is because there are only three possible π^* SRs at most as we have indicated. Consequently, when one considers the assignment of TASs, the core-excited resonances should also be taken into account.

To investigate the core-excited resonances, the energies of the excited states of the vertical anion of p-BQ were obtained with ωB97XD and M11 S-LC-TDDFT calculations using basis sets A1. Figure 3a-h shows the SPs for the ^2A_u, $^2B_{1u}$, $^2B_{2u}$, $^2B_{3u}$, ^2A_g, $^2B_{1g}$, $^2B_{2g}$ and $^2B_{3g}$ excited states solutions of the vertical p-BQ anion using the S-LC-TDDFT ωB97XD method with basis set A1. It is noteworthy that the eigenvalues in the S-LC-TDDFT calculations may consist of the following four solutions: (1) core-excited resonance, (2) the excitation of an electron to DC (E-DC) solutions, (3) SR, and (4) DC solutions. The 3rd and 4th solutions are the results of the excitation of an electron from the LUMO to higher lying virtual orbitals. Similar to those of SRs, the eigenvalues of the core-excited resonance solutions remain stable while those of the E-DC solutions change as α varies. Accordingly, TDDFT should be used with considerable caution for determining the energies of excited states. In Fig. 3a for the ^2A_u resonances, the 1st solution for $\alpha > 0.2$ and 5th solution for $\alpha > 1.9$ are primarily from the ^2A_u resonance solutions. Yet, the 2nd solution for $\alpha > 0.5$, 3rd for $\alpha > 0.6$, 4th for $0.8 < \alpha < 1.9$, and 5th for $0.8 < \alpha < 1.7$ correspond to the E-DC solutions. The 2nd solution for $0.2 < \alpha < 0.5$ and 4th for $0.6 < \alpha < 0.8$ correspond to the DC solutions. Five ACs are found in the SP. According to our observation, the first AC near $\alpha_{ac}(1,2) = 0.2$ is mainly from the couplings between 1^2A_u resonance and the first DC solutions. The 4th and 5th roots undergoing an AC near $\alpha_{ac}(4,5) = 1.9$ is from the couplings between 2^2A_u resonance and the E-DC solutions. The energy values acquired from the ACs are 2.78 eV at $\alpha_{ac}(1,2) = 0.2$ and 7.31 eV $\alpha_{ac}(4,5) = 1.9$, respectively. On the other hand, the 2nd–4th ACs near $\alpha_{ac}(2,3) = 0.5$, $\alpha_{ac}(3,4) = 0.6$, and $\alpha_{ac}(4,5) = 0.8$ are due to the couplings between E-DC and DC solutions. Hence, these spurious results need to be excluded. The SPs for other core-excited resonance states have been analysed in a similar manner as those of ^2A_u and they have been presented in Fig. 3b to 3h. For the $^2B_{1u}$ anion states, the acquired energies of the 1^2B_{1u}–3^2B_{1u} states are 5.27, 5.72, and 7.55 eV, respectively. For the $^2B_{2u}$ anion states, the acquired energies of the 1^2B_{2u}–3^2B_{2u} states are 2.99, 5.87, and 6.78 eV, respectively. For the $^2B_{3u}$ anion states, the acquired energies of the 1^2B_{3u}–5^2B_{3u} states are 3.49, 4.25, 5.48, 7.36, and 7.77 eV, respectively. For the ^2A_g anion states, the acquired energies of the 1^2A_g–3^2A_g states are 5.59, 5.96, and 7.17 eV, respectively. For the $^2B_{1g}$ anion states, the acquired energies of the 1^2B_{1g}–3^2B_{1g} states are 4.00, 6.04, and 7.02 eV, respectively. For the $^2B_{2g}$ anion states, the acquired energies of the 1^2B_{2g}–2^2B_{2g} states are 6.14 and 7.82 eV, respectively. For the $^2B_{3g}$ anion states, the acquired energies of the 1^2B_{3g}–4^2B_{3g} states are 2.86, 6.20, 6.54, and 7.47 eV, respectively.

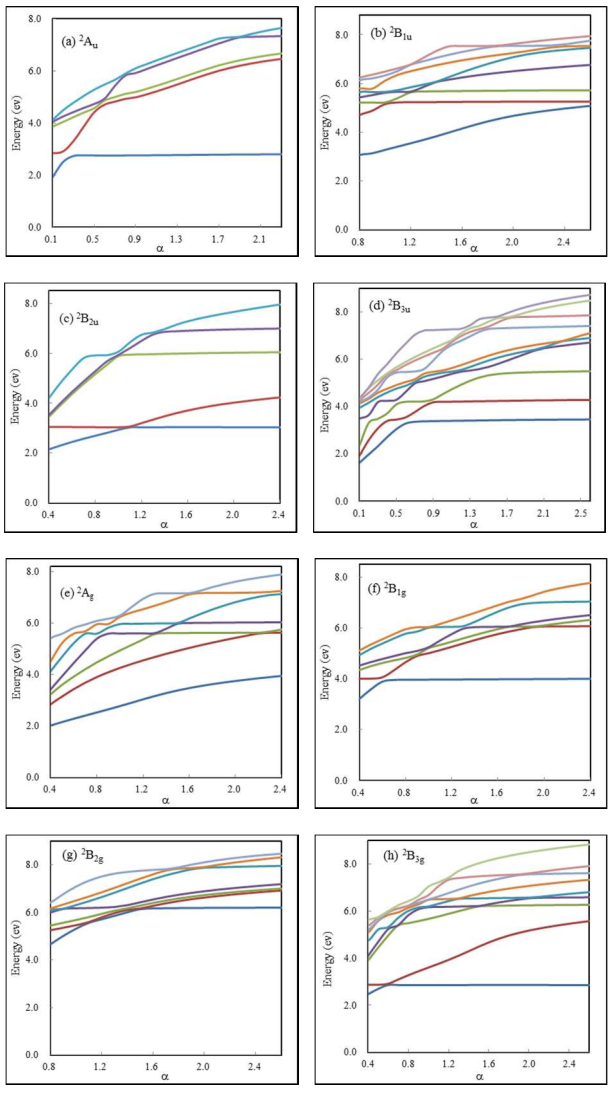

Fig. 3 SPs for vertical p-BQ radical anion via S-LC-TDDFT ωB97XD. Excitation energies for the (a) ^2A_u, (b) $^2B_{1u}$, (c) $^2B_{2u}$, (d) $^2B_{3u}$, (e) ^2A_g, (f) $^2B_{1g}$, (g) $^2B_{2g}$, and (h) $^2B_{3g}$ anion states as a function of α.

We then examine the characteristics of excited states for p-BQ vertical anion. Based on our analysis, the 1^2A_u state represents π^*_{LUMO}-π^* ($2b_{2g} \rightarrow 1a_u$) SR. The 1^2B_{3u} and 2^2B_{3u} states can be

ascribed to a mixture of the π-π* core-excited with π^*_{LUMO}-π* ($2b_{2g} \rightarrow 3b_{3u}$) shape resonances. The 1^2B_{2g} and 2^2B_{2g} states are mainly described by a mixture of the π-π* core-excited with π^*_{LUMO}-π* ($2b_{2g} \rightarrow 3b_{2g}$) shape resonances. The 1^2A_g-3^2A_g, 1^2B_{3g}-4^2B_{3g}, 1^2B_{1u}-3^2B_{1u}, and 1^2B_{2u}-3^2B_{2u} states can be ascribed to n-π*/σ-π* core-excitations. The 1^2B_{1g}-3^2B_{1g}, 3^2B_{3u}-5^2B_{1g}, and 2^2A_u states represent π-π* core-excited resonances.

Table 2 reports the energies of the excited states of p-BQ vertical anion via ωB97XD and M11 S-LC-TDDFT calculations using basis set A1. To compare with experimental results, the energies of the excited anion states relative to the ground neutral state are also included in the table. Accounting for a calculated vertical electron affinity of 1.90 eV, three electronic states, the 1^2A_u, 1^2B_{3g}, and 1^2B_{2u}, are possible candidates for the assignment of the resonances observed around 0.7 eV. With regard to the resonance detected around 1.4 eV, only the 1^2B_{3u} state has computed energy in this range. For the resonance observed around 2 eV, the 2^2B_{3u} and 1^2B_{1g} states are possible choices. As for the resonance observed around 4.37 and 5.8 eV, several π-π* (2^2B_{1g}, 1^2B_{2g}, 2^2B_{2g}, 2^2A_u, 4^2B_{3u}, and 5^2B_{3u}) and n-π*/σ-π* (2^2A_g, 2^2B_{3g}, 3^2B_{3g}, 4^2B_{3g}, and 3^2B_{1u}) possible states are predicted in the energy range. Among these, the 1^2B_{2g} and 2^2B_{2g} states have the same symmetry as the third $^2B_{2g}$ SR. Based on comparison between the experimental results observed in electron transmission spectroscopy and our calculations on p-BQ, the 0.69 eV feature is ascribed to 1^2A_u SR state which is derived from electron capture into $1a_u$ π^*_{CC} orbital. The 1.41 and 2.11 eV features are ascribed to the 1^2B_{3u}, and 2^2B_{3u} resonances that are the mixtures of shape ($3b_{3u}$ π^*_{CO}) and core-excited resonances. As for the 4.37 and 5.8 eV features, they are associated with the mixtures of shape ($3b_{2g}$ π_g^*) and core-excited resonances.

It is proper and fitting to comment here that the calculated energies inside the parentheses of Table 2 actually correspond to one of the following three possibilities: (a) SRs, (b) core-excited resonances, or (c) a mixture of both. While the calculated AEs for the three unbound π* TASs presented in Table 1 correspond to pure SRs, here in Table 2 they are more complicated. To illustrate, let us consider the case of pure SR in Table 2. The energy value obtained from ωB97XD S-LC-TDDFT method (0.88 eV) for pure 1^2A_u SR is in good agreement with the AE in Table 1 for $1a_u$ orbital obtained from SKT ωB97XD method (0.92 eV) when using the same A1 basis set. In addition, when core-excited resonances are taken into account, the experimental data around 1.35-1.43 and 4.2-4.37 eV which were not corresponding to any calculated SRs in Table 1 can now be assigned in Table 2.

For resonance parameters (E_R and Γ) of three π* SRs, the low lying 1^2A_u, 1^2B_{3g}, 1^2B_{2u}, 1^2B_{3u}, 1^2B_{1g}, and 2^2B_{3u} excited anion states, and the third SR related 1^2B_{2g}, and 2^2B_{2g} excited anion states, are all extracted from each AC via aforementioned (i,i,i) generalized Padé approximants. In case there are several ACs for one resonance state, the average values of E_R and Γ obtained from each set of resonance parameters are used. Table 3 reports the calculated resonance parameters for (a) SRs obtained by SKT ωB97XD, and (b) the vertical anion excited states of p-BQ obtained by S-LC-TDDFT ωB97XD calculations using basis set A1. Since generalized Padé approximant works best in the vicinity of ACs, the α range near α_{ac} is always used to extract E_R and Γ. In Table 3, the results of resonance parameters are reported from the average of four different calculations where each one is from the (3,3,3), (4,4,4) and (5,5,5) generalized Padé approximants employing slightly different E(α) data sets as input. As can be seen from the resonance energies of Table 3, our results are in agreement with those of the midpoint method. Next, for the resonance widths of SRs, our calculations of the resonance widths are 0.17, 0.35, and 1.76 eV using SKT ωB97XD for $1a_u$, $3b_{3u}$, and $3b_{2g}$ π* orbitals, respectively. Thus, their corresponding lifetimes are about 4, 2, and 0.4 fs for $1a_u$, $3b_{3u}$, and $3b_{2g}$ π* orbitals, respectively. As for the resonance widths of excited anion states, our calculations indicate the values are 0.35, 0.04, 0.01, 0.35, 0.06, 0.14, 0.40, and 0.38 eV for 1^2A_u, 1^2B_{3g}, 1^2B_{2u}, 1^2B_{3u}, 1^2B_{1g}, 2^2B_{3u}, 1^2B_{2g}, and 2^2B_{2g} anion states, respectively. Hence, the corresponding lifetimes are about 2-5 fs for the 1^2A_u, 1^2B_{3u}, 2^2B_{3u}, 1^2B_{2g} and 2^2B_{2g} SR associated TASs, and 11-47 fs for the 1^2B_{3g}, 1^2B_{2u} and 1^2B_{1g} core-excited states. Notice that the 1^2B_{3g}, 1^2B_{2u} and 1^2B_{1g} states correspond to Feshbach resonances. Thus, it is logical for them to have longer lifetimes than either SRs or a mixture of both resonances.

To sum up, the fundamental reasons for the success of our SKT LC-DFT and S-LC-TDDFT could be as follows. (1) The adoption of LC functionals can reduce the discontinuity of exchange-correlation potentials so that more reasonable energy gaps can be obtained[37a]. (2) The LC functionals can incorporate both relaxation and correlation effects appropriately.[37b] (3) The SM is invoked to distinct the unfilled orbital from the DC solutions.

4. Conclusion

The TASs of p-BQ have been studied by coupling the SM with DFT. Our calculation results can yield energies of shape and core-excited resonances in complete agreement with experimental data. For SRs, the SKT ωB97XD and M11 LC-DFT methods can efficiently generate better agreement in energy results when compared with S-EA SAC-CI and S-OVGF methods. As for core-excited resonances, the finding of using S-LC-TDDFT to distinguish them from the excitation of an electron to "virtual" DC solution is significant. More importantly, the proposed method can compute resonance lifetimes via analytic continuation method in conjunction with SPs. Thus, the previous experimental results of TASs for p-BQ have now been fully identified by taking into account of both SRs and core-excited resonances.

Acknowledgement

We would like to thank the referees for their valuable comments and suggestions during the revision process. This work was supported by Ministry of Science and Technology of Republic of China under the grant number MOST 103-2113-M-029 -003.

References and notes

[a] *Department of Chemistry, Tunghai University, 1727, Taiwan Boulevard Sec.4, Taichung 40704, Taiwan R.O.C. Fax: +886-4-23590426; Tel: +886-4-23590248-102; *E-mail: hycheng@thu.edu.tw*

1 R. Saini, N. Kaur and S. Kumar, *Tetrahedron*, 2014, **70**, 4285-4307.
2 R. A. Doong, C. C. Lee and C. M. Lien, *Chemosphere*, 2014, **97**, 54-63.

3 (a) B. Huskinson, S. Nawar, M. R. Gerhardt and M. J. Aziz, *ECS Trans.*, 2013, **53**, 101-105. (b) B. Huskinson, M. P. Marshak, C. Suh, S. Er, M. R. Gerhardt, C. J. Galvin, X. Chen, A. Aspuru-Guzik, R. G. Gordon and M. J. Aziz, *Nature*, 2014, **505**, 195-198.

4 (a) M. R. Gunner, J. Madeo and Z. Zhu, *J. Bioenerg. Biomembr.*, 2008, **40**, 509-519. (b) A. Osyczka, C. C. Moser, F. Daldal and P. L. Dutton, *Nature*, 2004, **427**, 607-612. (c) H. Nohl, W. Jordan and R. J. Youngman, *Adv. Free. Radic. Biol. Med.*, 1986, **2**, 211-279.

5 (a) M. A. Colucci, G. D. Couch and C. J. Moody, *Org. Biomol. Chem.*, 2008, **6**, 637-656. (b) S. P. Gupta, *Chem. Rev.*, 1994, **94**, 1507-1551.

6 G. J. Schulz, *Rev. Mod. Phys.*, 1973, **45**, 423-486.

7 (a) C. D. Cooper, W. T. Naff and R. N. Compton, *J. Chem. Phys.*, 2008, **63**, 2752-2757. (b) C. D. Cooper, W. F. Frey and R. N. Compton, *J. Chem. Phys.*, 1978, **69**, 2367-2374.

8 A. Modelli and P. D. Burrow, *J. Phys. Chem.*, 1984, **88**, 3550-3554.

9 (a) M. Allan, *Chem. Phys.*, 1983, **81**, 235-241. (b) M. Allan, *Chem. Phys.*, 1984, **84**, 311-319.

10 R. Pou-Amérigo, L. Serrano-Andrés, M. Merchán, E. Ortí and N. Forsberg, *J. Am. Chem. Soc.*, 2000, **122**, 6067-6077.

11 Y. Honda, M. Hada, M. Ehara and H. Nakatsuji, *J. Phys. Chem. A*, 2002, **106**, 3838-3849.

12 (a) J. Schiedt and R. Weinkauf, *J. Phys. Chem.*, 1999, **110**, 304-314. (b) D. A. Horke, Q. Li, L. Blancafort and J. R. Verlet, *Nat. Chem.*, 2013, **5**, 711-717.

13 (a) M. F. Falcetta and K. D. Jordan, *J. Phys. Chem.*, 1990, **94**, 5666-5669. (b) M. F. Falcetta and K. D. Jordan, *J. Am. Chem. Soc.*, 1991, **113**, 2903-2909. (c) M. F. Falcetta and K. D. Jordan, *Chem. Phys. Lett.*, 1999, **300**, 588-594. (d) M. F. Falcetta, Y. Choi and K. D. Jordan, *J. Phys. Chem. A*, 2000, **104**, 9605-9612. (d) C. Y. Juang and J. S. Y. Chao, *J. Phys. Chem.*, 1994, **98**, 13506-13512. (e) C. S. Chen, T. H. Feng and J. S. Y. Chao, *J. Phys. Chem.*, 1995, **99**, 8629-8632. (f) Y. H. Wei and H. Y. Cheng, *J. Phys. Chem. A*, 1998, **102**, 3560-3564.

14 (a) M. F. Falcetta, L. A. DiFalco, D. S. Ackerman, J. C. Barlow and K. D. Jordan, *J. Phys. Chem. A*, 2014, DOI: 10.1021/jp5003287. (b) K. D. Jordan, V. K. Voora and J. Simons, *Theor. Chem. Acc.*, 2014, **133**, 1-15.

15 (a) A. U. Hazi and H. S. Taylor, *Phys. Rev. A*, 1970, **1**, 1109-1120. (b) H. S. Taylor, *Adv. Chem. Phys.*, 1970, **18**, 91-147. (c) M. F. Fels and A. U. Hazi, *Phys. Rev. A*, 1972, **5**, 1236-1249. (d) H. S. Taylor and A. U. Hazi, *Phys. Rev. A*, 1976, **14**, 2071-2074.

16 T. Koopmans, *Physica*, 1934, **1**, 104-113.

17 W. Kohn and L. J. Sham, *Phys. Rev. A*, 1965, **140**, 1133-1138.

18 E. J. Baerends, O. V. Gritsenko and R. Van Meer, *Phys. Chem. Chem. Phys.,* 2013, **15**, 16408-16425.

19 (a) D. J.Tozer and F. De Proft, *J. Phys. Chem. A*, 2005, **109**, 8923-8929. (b) D. J. Tozer and F. De Proft, *J. Chem. Phys.*, 2007, **127**, 034108. (c) F. De Proft, N. Sablon, D. J. Tozer and P. Geerlings, *Farad. Discuss.*, 2007, **135**, 151-159. (d) N. Sablon, F. De Proft, P. Geerlingsa and D. J. Tozer, *Phys. Chem. Chem. Phys.*, 2007, **9**, 5880-5884. (e) A. M. Teale, F. De Proft and D. J. Tozer, *J. Chem. Phys.*, 2008, **129**, 044110. (f) B. Hajgató, M. S. Deleuze, D. J. Tozer and F. De Proft, *J. Chem. Phys.*, 2008, **129**, 084308. (g) M. J. G. Peach, F. De Proft and D. J. Tozer, *J. Phys. Chem. Lett.*, 2010, **1**, 2826-2831. (h) A. Borgoo and D. J. Tozer, *J. Phys. Chem. A*, 2012, **116**, 5497-5500. (i) A. M.Teale, F. De Proft, P. Geerlings and D. J. Tozer, *Phys. Chem. Chem. Phys.*, 2014, **16**, 14420-14434.

20 (a) H. Y. Cheng and C. C. Shih, *J. Phys. Chem. A*, 2009, **113**, 1548-1554. (b) H. Y. Cheng, C. C. Shih and J. T. Chang, *J. Phys. Chem. A*, 2009, **113**, 9551-9558. (c) H. Y. Cheng, J. T. Chang and C. C. Shih, *J. Phys. Chem. A,* 2010, **114**, 2920-2929. (d) H. Y. Cheng, C. W. Chen, J. T. Chang and C. C. Shih, *J. Phys. Chem. A*, 2010, **115**, 84-93. (e) H. Y. Cheng and C. W. Chen, *J. Phys. Chem. A*, 2011, **115**, 10113-10121. (f) H. Y. Cheng, C. W. Chen and C. H. Huang, *J. Phys. Chem. A*, 2012, **116**, 3224-3236. (g) H. Y. Cheng and C. W. Chen, *J. Phys. Chem. A*, 2012, **116**, 12364-12372. (h) H. Y. Cheng, Y. S. Huang and P. Q. Huang, *J. Chin. Chem. Soc.*, 2014, to be published. (i) Y. Yokoi, K. Kano, Y. Minoshima and T. Takayanagi, *Comp. Theor. Chem.*, 2014, **1046**, 99-106.

21 (a) A. Modelli and P. D. Burrow, *Phys. Chem. Chem. Phys.*, 2009, **11**, 8448-8455. (b) S. A. Pshenichnyuk, A. S.Vorob'ev and A. Modelli, *J. Chem. Phys.*, 2011, **135**, 184301.

22 C. E. Check, T. O. Faust, J. M. Bailey, B. J. Wright, T. M. Gilbert and L. S. Sunderlin, *J. Phys. Chem. A*, 2001, **105**, 8111−8116.

23 (a) T. H. Dunning Jr., *J. Chem. Phys.*, 1989, **90**, 1007-1023. (b) R. A. Kendall, T. H. Dunning Jr. and R. J. Harrison, *J. Chem. Phys.*, 1992, **96**, 6796-6806.

24 P. D. Burrow, A. E. Howard, A. R. Johnston and K. D. Jordan, *J. Phys. Chem.*, 1992, **96**, 7570-7578.

25 The resonance parameters can also be computed by means of density-of-state method. (V. A. Mandelshtam, T. R. Ravuri, H. S. Taylor, *Phys. Chem. Lett.*, 1993, **70**, 1932-1935.)

26 (a) W. H. Miller and T. F. George, *J. Chem. Phys.*, 1972, **56**, 5668-5681. (b) T. F. George and K. Morokuma, *Chem. Phys.*, 1973, **2**, 129-136. (c) C. W. McCurdy and J. F. McNutt, *Chem. Phys. Lett.*, 1983, **94**, 306-310. (d) A. D. Isaacson and D. G. Truhlar, *Chem. Phys. Lett.*, 1984, **110**, 130-134. (e) R. F. Frey and J. Simons, *J. Chem. Phys.*, 1986, **84**, 4462-4469. (f) M. Garcia-Sucre and R. Lefebvre, *Chem. Phys. Lett.*, 1986, **130**, 240-244. (g) L. Yu and J. S. Y. Chao, *J. Chin. Chem. Soc.*, 1993, **40**, 11-22. (h) K. D. Jordan, *Chem. Phys.*, 1975, **9**, 199-204. (i) K. D. Jordan, *J. Mol. Spectrosc.*, 1975, **56**, 329−331. (j) J. S. Y. Chao, M. F. Falcetta and K. D. Jordan, *J. Chem. Phys.*, 1990, **93**, 1125-1135.

27 J. D. Chai and M. Head-Gordon, *Phys. Chem. Chem. Phys.*, 2008, **10**, 6615-6620.

28 R. Peverati and D. G. Truhlar, *J. Phys. Chem. Lett.*, 2011, **2**, 2810-2817.

29 L. Goerigk and S. Grimme, *J. Chem. Theory Comput.,* 2011, **7**, 291-309.

30 (a) N. Nakatsuji, *Chem. Phys. Lett.*, 1978, **59**, 362-364. (b) H. Nakatsuji, *Chem. Phys. Lett.*, 1979, **67**, 329-333. (c) H. Nakatsuji and K. Hirao, *J. Chem. Phys.*, 1978, **68**, 2053-2065. (d) Y. Ohtsuka, P. Piecuch, J. R. Gour, M. Ehara and H. Nakatsuji, *J. Chem. Phys.*, 2007, **126**, 164111.

31 (a) L. S. Cederbaum and W. Domcke, *Adv. Chem. Phys.*, 1977, **36**, 205-344. (b) W. von Niessen, J. Schirme and L. S. Cederbaum, *Comput. Phys. Rep.*, 1984, **1**, 57-125. (c) J. V. Ortiz, *J. Chem. Phys.*, 1988, **89**, 6348-6352. (d) V. G. Zakrzewski and W. von Niessen, *J. Comput. Chem.*, 1993, **14**, 13-18. (e) V. G. Zakrzewski and J. V. Ortiz, *Int. J. Quant. Chem.*, 1995, **53**, 583-590.

32 M. Nooijen and R. J. Bartlett, *J. Chem. Phys.*, 1995, **102**, 3629−3647.

33 According to our stabilization calculations on the $^2\Pi_g$ anion state of N_2, the resonance parameters obtained by EA SAC-CI are very close to those by EA EOM-CCSD when using the same basis sets. However, the former method is computationally more efficient than the latter one.

34 It is because that TD ωB97XD has the best performance among several TD LCDFT methods for the calculation of excitation energies. In addition, it has quantatatively better overall performance for some excited states than the SAC-CI approach. (M. Alipour, *J. Phys. Chem. A*, 2014, ***118***, 1741-1747.)

35 M. J. Frisch, G. W. Trucks, H. B. Schlegel, G. E. Scuseria, M. A. Robb, J. R. Cheeseman, G. Scalmani, V. Barone, B. Mennucci, G. A. Petersson, H. Nakatsuji, M. Caricato, X. Li, H. P. Hratchian, A. F. Izmaylov, J. Bloino, G. Zheng, J. L. Sonnenberg, M. Hada, M. Ehara, K. Toyota, R. Fukuda, J. Hasegawa, M. Ishida, T. Nakajima, Y. Honda, O. Kitao, H. Nakai, T. Vreven, J. A. Montgomery, Jr., J. E. Peralta, F. Ogliaro, M. Bearpark, J. J. Heyd, E. Brothers, K. N. Kudin, V. N. Staroverov, T. Keith, R. Kobayashi, J. Normand, K. Raghavachari, A. Rendell, J. C. Burant, S. S. Iyengar, J. Tomasi, M. Cossi, N. Rega, J. M. Millam, M. Klene, J. E. Knox, J. B. Cross, V. Bakken, C. Adamo, J. Jaramillo, R. Gomperts, R. E. Stratmann, O. Yazyev, A. J. Austin, R. Cammi, C. Pomelli, J. W. Ochterski, R. L. Martin, K. Morokuma, V. G. Zakrzewski, G. A. Voth, P. Salvador, J. J. Dannenberg, S. Dapprich, A. D. Daniels, O. Farkas, J. B. Foresman, J. V. Ortiz, J. Cioslowski and D. J. Fox, *Gaussian 09, Revision D.01*. Gaussian, Inc., Wallingford CT, 2013.

36 K. Hagen and K. Hedberg, *J. Chem. Phys.*, 1973, **59**, 158-162.

37 (a) T. Tsuneda, J. W. Song, S. Suzuki and K. Hirao, *J. Chem. Phys.*, 2010, **133**, 174101. (b) R. Kar, J. W. Song and K. Hirao, *J. Comput. Chem.*, 2013, **34**, 958-964.

Table 1 Calculated AEs (eV) for p-Benzoquinone

method	basis set	$2b_{2g}$	$1a_u$		$3b_{3u}$		$3b_{2g}$
SKT ωB97XD	A1	-2.06	0.92		1.98		5.43
	A2	-2.05	0.87		1.95		5.43
	B1	-1.97	0.89		1.90		5.70
	B2	-1.97	0.85		1.85		5.40
	C1	-1.98	0.89		1.90		5.52
	C2	-1.98	0.88		1.92		5.61
SKT M11	A1	-1.88	0.93		2.09		5.89
	B1	-1.77	0.96		2.19		5.89
	C1	-1.78	0.90		2.18		5.85
SKT B2PLYPD3	A1	-2.24	0.59		1.70		5.82
	B1	-2.24	0.57		1.85		5.65
	C1	-2.23	0.49		1.64		5.51
S-EA SAC-CI	A1	-1.21	1.27		2.31		5.99
	A2	-1.16	1.14		2.29		5.98
	B1	-1.19	1.22		2.30		5.99
	B2	-1.21	1.14		2.32		6.02
S-OVGF	A1	-1.03	2.05		3.37		6.91
	B1	-1.04	2.05		3.14		7.27
	C1	-1.21	1.80		2.87		7.10
expt [a]		-1.89	0.70 (b_{3u})	1.35 (a_u)	1.90 (b_{3u})	4.35 (c.e.)[f]	
expt [b]			0.69 (b_{3u})	1.41 (a_u)	2.11 (c.e.)[f]	4.37 (b_{2g})	~5.8
expt [c]			0.72 (b_{3u})	1.43 (a_u)	2.15 (b_{3u})	4.2	~5.4
theory [d]		-1.64	0.91 (a_u)	1.31 (b_{3u})	1.87 (b_{3u})		
theory [e]		-1.57	0.83 (a_u)	1.79 (b_{3u})	2.44 (b_{3u})		

[a] ref 7. [b] ref 8. [c] ref 9. [d] ref 10. [e] ref 11. [f] core-excited resonance.

Cite this: DOI: 10.1039/c0xx00000x

www.rsc.org/xxxxxx

ARTICLE TYPE

Table 2 Energies [a] (eV) of the excited states of p-BQ vertical anion obtained by ωB97XD and M11 S-LC-TDDFT calculations using basis set A1

Excited state	main contribution	nature	ωB97XD	M11	Expt [b]	Expt [c]	Expt [d]	Expt [e]	Theory [f]	Theory [g]
1^2A_u	$2b_{2g} \rightarrow 1a_u$	π*-π*	2.78 (0.88)	2.66 (0.76)	0.70	0.69	0.72	0.77	0.91	0.83
1^2B_{3g}	$4b_{3g} \rightarrow 2b_{2g}$	n-π*	2.86 (0.96)	2.72 (0.82)					0.87	
1^2B_{2u}	$5b_{2u} \rightarrow 2b_{2g}$	n-π*	2.99 (1.09)	2.95 (1.05)					0.96	
1^2B_{3u}	$2b_{2g} \rightarrow 3b_{3u}$	π*-π*	3.49 (1.59)	3.30 (1.40)	1.35	1.41	1.43	1.6	1.31	1.79
	$2b_{3u} \rightarrow 2b_{2g}$	π-π*								
1^2B_{1g}	$1b_{1g} \rightarrow 2b_{2g}$	π-π*	4.00 (2.10)	3.94 (2.04)					1.99	
	$2b_{3u} \rightarrow 1a_u$	π-π*								
2^2B_{3u}	$2b_{3u} \rightarrow 2b_{2g}$	π-π*	4.25 (2.35)	4.25 (2.35)	1.90	2.11	2.15	2.0	1.87	2.44
	$1b_{1g} \rightarrow 1a_u$	π-π*								
	$2b_{2g} \rightarrow 3b_{3u}$	π*-π*								
1^2B_{1u}	$4b_{3g} \rightarrow 1a_u$	n-π*	5.27 (3.37)	5.31 (3.41)						
3^2B_{3u}	$1b_{1g} \rightarrow 1a_u$	π-π*	5.48 (3.58)	5.46 (3.56)						
	$1b_{3u} \rightarrow 2b_{2g}$	π-π*								
1^2A_g	$5b_{2u} \rightarrow 1a_u$	n-π*	5.59 (3.69)	5.96 (4.06)						
2^2B_{1u}	$4b_{3g} \rightarrow 1a_u$	n-π*	5.72 (3.82)	5.81 (3.91)						
2^2B_{2u}	$4b_{3g} \rightarrow 3b_{3u}$	n-π*	5.87 (3.97)	5.80 (3.90)						
2^2A_g	$5b_{2u} \rightarrow 1a_u$	n-π*	5.96 (4.06)	6.07 (4.17)						
2^2B_{1g}	$2b_{3u} \rightarrow 1a_u$	π-π*	6.04 (4.14)	6.34 (4.44)						
	$1b_{1g} \rightarrow 2b_{2g}$	π-π*								
1^2B_{2g}	$1b_{2g} \rightarrow 2b_{2g}$	π-π*	6.14 (4.24)	6.35 (4.45)	4.35	4.37	4.2	4.2		
	$2b_{3u} \rightarrow 3b_{3u}$	π-π*								
	$2b_{2g} \rightarrow 3b_{2g}$	π*-π*								
2^2B_{3g}	$5b_{2u} \rightarrow 3b_{3u}$	n-π*	6.20 (4.30)	6.21 (4.31)						
3^2B_{3g}	$3b_{3g} \rightarrow 2b_{2g}$	σ-π*	6.54 (4.64)	6.48 (4.58)						
3^2B_{2u}	$4b_{3g} \rightarrow 3b_{3u}$	n-π*	6.78 (4.88)	7.11 (5.21)						
3^2B_{1g}	$2b_{3u} \rightarrow 1a_u$	π-π*	7.02 (5.12)	7.31 (5.41)						
3^2A_g	$8a_g \rightarrow 2b_{2g}$	σ-π*	7.17 (5.27)	7.18 (5.28)						
4^2B_{3u}	$1b_{1g} \rightarrow 1a_u$	π-π*	7.36 (5.46)	7.49 (5.59)						
	$1b_{3u} \rightarrow 2b_{2g}$	π-π*								
2^2A_u	$1b_{1g} \rightarrow 3b_{3u}$	π-π*	7.31 (5.41)	7.48 (5.58)						
4^2B_{3g}	$5b_{2u} \rightarrow 3b_{3u}$	n-π*	7.47 (5.57)	7.99 (6.09)						
	$3b_{3g} \rightarrow 2b_{2g}$	σ-π*								
3^2B_{1u}	$7b_{1u} \rightarrow 2b_{2g}$	σ-π*	7.55 (5.65)	7.57 (5.67)						
	$1b_{3u} \rightarrow 2b_{2g}$	π-π*								
5^2B_{3u}	$1b_{1g} \rightarrow 1a_u$	π-π*	7.77 (5.87)	7.53 (5.63)						
	$1b_{2g} \rightarrow 3b_{3u}$	π-π*								
2^2B_{2g}	$2b_{3u} \rightarrow 3b_{3u}$	π-π*	7.82 (5.92)	7.98 (6.08)		~5.8				
	$1b_{2g} \rightarrow 2b_{2g}$	π-π*								
	$2b_{2g} \rightarrow 3b_{2g}$	π*-π*								

[a] The values in parentheses are energies of the excited anion states relative to the ground neutral state. [b] ref 7. [c] ref 8. [d] ref 9a. [e] ref 9b. [f] ref 10. [g] ref 11.

Table 3 Resonance parameters (eV) for (a) SRs obtained by SKT ωB97XD and (b) the vertical anion excited states of p-BQ obtained by S-LC-TDDFT ωB97XD calculations

		E_R	□Γ
SRs	$1a_u$ π*	0.958	0.170
	$3b_{3u}$ π*	1.955	0.345
	$3b_{2g}$ π*	5.536	1.760
Excited States [a]	1^2A_u	0.910	0.346
	1^2B_{3g}	0.956	0.042
	1^2B_{2u}	1.136	0.014
	1^2B_{3u}	1.587	0.351
	1^2B_{1g}	2.099	0.058
	2^2B_{3u}	2.332	0.139
	1^2B_{2g}	4.410	0.397
	2^2B_{2g}	5.910	0.375

[a] The values of E_R are the energies of vertical anion excited states relative to the ground neutral state.

Graphical Abstract for Table of Content

The energies and lifetimes of shape and core-excited resonances of p-benzoquinone have been studied in this paper. The obtained resonance parameters are of fundamental importance in understanding the bonding and electronic processes of quinones.